
Analytical Solution to the Zonal Harmonics Problem Using Koopman Operator Theory

David Arnas*, Richard Linares†

Abstract

This work introduces the use of the Koopman Operator Theory to generate analytical solutions for the zonal harmonics problem of a satellite orbiting a non spherical celestial body. Particularly, the solution proposed directly provides the osculating evolution of the system and can be automated to generate any approximation order to the solution. Moreover, this manuscript defines a modified set of orbital elements that can be applied to any kind of orbit and that allows the Koopman Operator to generate stable and accurate solutions. In that regard, several examples of application are included, showing that the proposed methodology can be used in any kind of orbit, including circular, elliptic, parabolic and hyperbolic orbits.

1 Introduction

The study of the effects in the motion of satellites subjected to the zonal harmonic components of the gravitational potential of an oblate planet is one of the most elemental problems in celestial mechanics and is of great importance both for the design and control of space missions. However, despite being this problem one of the most simple models to study in astrodynamics (apart from the Keplerian motion), the problem is known to have no analytical solution [1, 2], and thus, a wide variety of approaches have appeared over the years to provide approximate solutions to this problem [3, 4, 5, 6, 7, 8, 9, 10, 11, 12, 13, 14, 15]. In this regard, the analytic and semi-analytic solutions are of special interest since they allow us to have a deeper understanding of the problem, to obtain a faster long term propagation of orbiting objects, to analyze the stability of orbits [16, 17, 18], or to define and assess satellite constellations [19, 20, 21] and formation flying [22, 23, 24, 25] among other topics.

Among the zonal terms of the gravitational potential, the the main satellite problem (the study of the motion of a satellite subjected to the J_2 term

*Massachusetts Institute of Technology, MA, USA. Email: ARNAS@MIT.EDU

†Massachusetts Institute of Technology, MA, USA. Email: LINARES@MIT.EDU

of the Earth gravitational potential) has always been of special importance as it is the most important gravitational perturbation for satellites orbiting the Earth. Examples of that include the solutions proposed by Brouwer [3], Kozai [4], Deprit [6], or Liu [7], which are still extensively used both in theoretical and applied problems. Particularly, Brouwer [3], based on the von Zeipel perturbation method, proposed a first order solution which was later complemented by Lyddane [26] and Cohen [27] to study orbits with either small eccentricity or inclination, and by Coffey [28] to be able to effectively assess orbits close to the critical inclination. Kozai [4] proposed, on the other hand, a different approach based on the decomposition of the motion in first-order secular, second-order secular, short-periodic, and long-periodic terms. Afterwards, he extended Brouwer's formulation by introducing a second order solution [5] to the main satellite problem. Later, Deprit [6] approached the problem differently by making use of Lie series to define a set of canonical mappings that allows to generate an approximate solution following an iterative set of transformations [29]. This methodology led to the Lie-Deprit methods, a set of perturbation techniques that has been extensively used in the literature to deal with the main satellite problem [29, 30, 31, 32, 33, 34, 35, 36, 37]. Important examples of application of this approach include the method of elimination of the parallax [8], or the elimination of the perigee [11].

In this work, we approach the problem from a different perspective. Instead of performing near unitary transformations using a small parameter, we make use of operator theory to generate solutions to this problem directly. Operator theory is based on functional analysis [38] and focus on the study of linear operators in functional spaces [39]. Operator theory is widely used in theoretical Physics [40] (specially in quantum mechanics) and other research fields [41, 42] such as Fluid-dynamics [43] or control [44, 45, 46], but is not widely used in astrodynamics. Particularly, this manuscript focuses on the use of the Koopman operator, a linear operator introduced by Koopman [47] and later developed by Newmann [48] that is able to transform a non-linear system in a finite number of dimensions into a linear system in an infinite number of dimensions, on the zonal harmonics problem around an oblate celestial body. This allows to linearize the system (benefiting from the interesting properties of linear systems) while obtaining a good approximation to the solution. The Koopman operator has already been proposed to study problems in celestial mechanics, particularly the motion around libration points in the 3rd body problem [49], and attitude dynamics [50], but it has never been successfully applied to the zonal harmonics problem around a celestial body.

To that end, this work presents the methodology to apply the Koopman operator to the zonal harmonics problem. To be more precise, the contributions of this work are as follows; 1) a new set of orbital elements is developed based on Arnas [51], 2) the development of a closed-form computation of the

Koopman matrix using Legendre polynomials, 3) numerical error analysis of the analytical Koopman-based solution applied to the motion of a satellite orbiting a non-spherical celestial body. Particularly, this manuscript makes use of a modified set of orbital elements from Arnas [51] especially devised for their application alongside the Koopman operator. This set of orbital elements is able to represent any kind of orbit, including circular, elliptic, parabolic and hyperbolic orbits. In that regard, several examples of application are included to show the performance of the methodology for different orbits. Additionally, this work proposes the use of Legendre polynomials to compute the Koopman matrix of the system. This provides several advantages, including lower computation complexity, easier implementation, and a better distribution of the error in the variable range defined.

This manuscript is organized as follows. First, we include a summary of the Koopman operator theory and the methodology followed to apply it to the zonal harmonics problem. Second, we propose two sets of orbital elements to represent the dynamical system. The particularity of these sets of orbital elements is that they allow us to represent the differential equation governing the system in completely polynomial form, being, in addition, their expressions cuasi-linear for the application of the Koopman operator methodology. These set of orbital elements are a set of variables especially devised for their use with the Koopman operator due to their particular properties. Third, we apply this methodology to a collection of four common orbits used in astrodynamics, namely, a sun-synchronous frozen orbit, a molniya orbit, a hyperbolic orbit, and a near equatorial orbit. This allows us to show the performance of the methodology presented in this work and its possibilities.

2 Koopman operator theory

We depart from the classical initial value problem, represented by an autonomous system of differential equations expressed as:

$$\begin{cases} \frac{d}{dt}\mathbf{x}(t) = \mathbf{f}(\mathbf{x}) \\ \mathbf{x}(t_0) = \mathbf{x}_0 \end{cases} ; \quad (1)$$

where $\mathbf{x} \in \mathbb{R}^d$ is the set of d variables that evolves with time t and that define the state of the system. In here, $\mathbf{f} : \mathbb{R}^d \rightarrow \mathbb{R}^d$ represents the mathematical model of a given dynamical system, d is the number of dimensions of the problem, and \mathbf{x}_0 are the initial conditions.

Let $g(\mathbf{x})$ be an observable of the space, or in other words, $g(\mathbf{x})$ is a function in the set of variables \mathbf{x} . Then, if we study the evolution of $g(\mathbf{x})$ in the dynamic defined by Eq. (1) we obtain:

$$\frac{d}{dt}g(\mathbf{x}) = \mathcal{K}(g(\mathbf{x})) = (\nabla_{\mathbf{x}}g(\mathbf{x})) \frac{d}{dt}\mathbf{x}(t) = (\nabla_{\mathbf{x}}g(\mathbf{x})) \mathbf{f}(\mathbf{x}), \quad (2)$$

where $\nabla_{\mathbf{x}}g = [\partial g/\partial x_1, \partial g/\partial x_2, \dots, \partial g/\partial x_d]$, and $\mathcal{K}(g(\mathbf{x}))$ is defined as the Koopman operator applied to an observable. This means that the evolution of any observable under the effects of the dynamical system is provided by the Koopman operator:

$$\mathcal{K}(\cdot) = (\nabla_{\mathbf{x}}\cdot) \mathbf{f}(\mathbf{x}). \quad (3)$$

where $(\nabla_{\mathbf{x}}\cdot) = [\partial(\cdot)/\partial x_1, \partial(\cdot)/\partial x_2, \dots, \partial(\cdot)/\partial x_d]$. At this point, it is important to note that since the Koopman operator was generated applying the chain rule in the derivative of the observable, the operator is in fact linear [47], and thus:

$$\mathcal{K}(C_1g_1(\mathbf{x}) + C_2g_2(\mathbf{x})) = C_1\mathcal{K}(g_1(\mathbf{x})) + C_2\mathcal{K}(g_2(\mathbf{x})), \quad (4)$$

where C_1 and C_2 are two constants.

The main idea of the Koopman operator methodology is to find an approximated linear representation of the full dynamical system, and then use the property of linearity to obtain the exact solution to this approximation. To that end, the Koopman operator makes use of an extended configuration space of dimension $m > d$ that is able to approximate the non-linearities of the original system. In fact, if we could be able to work with the complete infinite Hilbert space [44], that is, a configuration space in an infinite number of dimensions, the nonlinearities of the system would be completely represented by this linear operator. However, since we are constrained by the use of a limited set of dimensions in the extended space, the linearization only provides an approximation of the original system that is better the closer is the system in the extended space to a linear one.

In order to perform this linearization, this manuscript makes use of the Garlekin method to obtain an approximated linearized system of equations. The Garlekin method is based on the idea of performing this approximation by finding the projection of the original system into a set of orthogonal functions that define the extended space of configuration for the Koopman operator. This projection is performed using inner products between functions. Particularly, let $f(\mathbf{x})$ be the function to represent in the dynamic, and let $g(\mathbf{x})$ be a basis function. Then, the inner product between both functions is represented by:

$$\langle f, g \rangle = \int_{\Xi} f(\mathbf{x})g(\mathbf{x})w(\mathbf{x})d\mathbf{x}, \quad (5)$$

where $w(\mathbf{x})$ is a weighting associated with the basis functions, and Ξ is the domain in which the basis functions are defined. That way, the error resultant in the approximation is orthogonal to the configuration space defined by the set of basis functions. Therefore, a set of orthogonal basis functions has to be defined in the extended space of dimension m . To that end, this work makes use of Legendre polynomials as basis functions. The reason for that is the multiple advantages that they provide when computing the inner

products. First, they are polynomials, which simplifies the computation. Second, Legendre polynomials are defined in a bounded domain $([-1, 1])$ as opposed to other basis functions, like Hermite polynomials, which are defined in all \mathbb{R} . Third, their weighting function is a constant, a fact that simplifies the expression of the inner product. This allows to ease the automatized computation of all the inner products required in the methodology.

Let $\mathbf{L}(\mathbf{x})$ be the set of all the basis functions of the problem in the original variables written in vector form $L(\mathbf{x}) = [L_1(\mathbf{x}), \dots, L_m(\mathbf{x})]^T$, where $L_i(\mathbf{x})$ represents the basis function i from the set. Then, the derivative of a basis function $L_i(\mathbf{x})$ can be obtained using the Koopman operator:

$$\mathcal{K}(L_i) = \frac{d}{dt}L_i = (\nabla_{\mathbf{x}}L_i) \mathbf{f}, \quad (6)$$

where it is important to note that $\nabla_{\mathbf{x}}L_i(\mathbf{x})$ can be represented by a combination of basis functions from $\mathbf{L}(\mathbf{x})$ due to the orthogonality and polynomial nature of the basis functions. Therefore, our objective now is to approximate this derivative with the basis functions defined in $L(\mathbf{x})$. This is done using the inner product operation. Let K be the Koopman matrix, a matrix of size $m \times m$ whose components K_{ij} contain the value of the projection of the derivative of the basis function i into the basis function j . In other words:

$$K_{ij} = \langle (\nabla_{\mathbf{x}}L_i) \mathbf{f}, L_j \rangle = \int_{\Xi} (\nabla_{\mathbf{x}}L_i) \mathbf{f} L_j w d\mathbf{x}. \quad (7)$$

For this work, these inner products are always performed between polynomials, and thus, it is possible to directly compute the integral analytically which significantly improves the computational speed of the methodology presented. Then, by following this procedure for all the combinations of basis functions, a linear system in the form:

$$\frac{d}{dt}\mathbf{L} = K\mathbf{L}. \quad (8)$$

is generated, which represents the approximated linear problem of the dynamic. Note that by using higher orders of basis functions, the Koopman matrix increases in size, but it is better able to better represent the nonlinearities of the original system.

Once this linearization is performed, it is only required to solve the linear system represented by Eq. (8). This can be done, for instance, using the spectral theorem when the matrix K is diagonalizable. In particular, let E_i and \mathbf{v}_i be the eigenvalues and corresponding left eigenvectors of the matrix K . In addition, let V be the matrix containing all the left eigenvectors in its rows. Then, by pre-multiplying V in Eq. (8) we obtain:

$$V \frac{d}{dt}\mathbf{L} = EK\mathbf{L} = EV\mathbf{L}, \quad (9)$$

where E is a diagonal matrix containing all the eigenvalues of the system. We know that V is a constant matrix since it is composed by the eigenvectors of the system, therefore:

$$V \frac{d}{dt} \mathbf{L} = \frac{d}{dt} (V\mathbf{L}) = EV\mathbf{L}, \quad (10)$$

where we can perform the algebraic variable transformation $\Phi = V\mathbf{L}$ with $\phi_i = \mathbf{v}_i \mathbf{L}$, called the Koopman Canonical Transform [45], to obtain:

$$\frac{d}{dt} \Phi = E\Phi, \quad (11)$$

whose solution is:

$$\Phi(t) = \exp(Et)\Phi(t_0). \quad (12)$$

In this regard, it is important to note that the functions $\Phi = V\mathbf{L}$ are in fact the eigenfunctions of the space defined by the dynamical system or, in other words, they are the set of functions defining the orthogonal directions of the Hilbert space of dimension m subjected to the dynamic of the system.

The objective is now to recuperate the original variables from the system. From Eq. (12) we can obtain the evolution of the basis functions L :

$$\mathbf{L}(t) = V^{-1}\Phi = V^{-1} \exp(Et)V\mathbf{L}(t_0). \quad (13)$$

In addition, the original variables \mathbf{x} can be represented using the basis functions \mathbf{L} through a projection on this basis. Let T be a transformation matrix of size $d \times m$ defined as:

$$T_{ij} = \langle x_i, L_j \rangle = \int_{\Xi} x_i L_j w d\mathbf{x}, \quad (14)$$

that is, the component T_{ij} represents the projection of the original variable x_i with $i \in \{1, \dots, d\}$ into the basis function j with $j \in \{1, \dots, m\}$. T is also called the Koopman modes matrix since it relates the original variables from the problem with the eigendecomposition of the dynamic, and thus, the frequencies of the motion. Therefore, the original set of variables $\mathbf{x}(t)$ can be expressed as:

$$\mathbf{x}(t) = T\mathbf{L}(t) = TV^{-1} \exp(Et)V\mathbf{L}(\mathbf{x}_0), \quad (15)$$

where \mathbf{x}_0 are the initial conditions of the original set of variables.

3 Zonal formulation

In order to efficiently apply the Koopman operator to a perturbed system, we require that the system behaves like a linear system with a small perturbation. This is due to the fact that for a real application of the Koopman

operator we can only use a limited number of basis functions, and thus, the closer we are to the linear system, the faster the perturbation method will converge to the solution of the problem. Therefore, we require a formulation that is able to fully represent the zonal harmonics perturbation in the system and that is close to linear for the solution to converge quickly. In that regard, Ref [51] introduced a new set of orbital elements that fulfills the conditions we are looking for. However, due to the particularities of the Koopman operator methodology, some modifications to that formulation have to be performed. For that reason, we include a summary of the formulation presented in Ref [51] as a reference for this manuscript.

The Hamiltonian in spherical coordinates of a satellite orbiting the Earth and subjected to the zonal harmonics terms of the gravitational perturbation is:

$$\mathcal{H} = \frac{1}{2} \left(p_r^2 + \frac{p_\varphi^2}{r^2} + \frac{p_\lambda^2}{r^2 \cos^2(\varphi)} \right) - \frac{\mu}{r} \left(1 - \sum_{n=2}^m J_n P_n(\sin(\varphi)) \frac{R_\oplus^n}{r^n} \right), \quad (16)$$

where μ is the gravitational constant of the Earth, R_\oplus is the Earth Equatorial radius, r is the radial distance from the satellite to the center of the Earth, φ is the latitude, λ is the longitude of the satellite in the inertial frame of reference for a given instant, J_n are the zonal terms of the Earth gravitational potential, and $P_n(\sin(\varphi))$ are the Legendre polynomials of order n applied to the variable $\sin(\varphi)$. In addition, the conjugate momenta of these variables are:

$$\begin{aligned} p_r &= \dot{r}; \\ p_\varphi &= r^2 \dot{\varphi}; \\ p_\lambda &= r^2 \cos^2(\varphi) \dot{\lambda}; \end{aligned} \quad (17)$$

where we defined \dot{x} as the derivative with respect to time of variable x . The associated Hamilton equations of this hamiltonian are:

$$\begin{aligned} \frac{dr}{dt} &= p_r; \\ \frac{dp_r}{dt} &= -\frac{\mu}{r^2} + \frac{p_\varphi^2}{r^3} + \frac{p_\lambda^2}{r^3 \cos^2(\varphi)} + \sum_{n=2}^m (n+1) \mu J_n P_n(\sin(\varphi)) \frac{R_\oplus^n}{r^{n+2}}; \\ \frac{d\varphi}{dt} &= \frac{p_\varphi}{r^2}; \\ \frac{dp_\varphi}{dt} &= -\frac{p_\lambda^2 \sin(\varphi)}{r^2 \cos^3(\varphi)} - \sum_{n=2}^m \mu J_n \frac{\partial P_n(\sin(\varphi))}{\partial \varphi} \frac{R_\oplus^n}{r^{n+1}}; \\ \frac{d\lambda}{dt} &= \frac{p_\lambda}{r^2 \cos^2(\varphi)}; \\ \frac{dp_\lambda}{dt} &= 0. \end{aligned} \quad (18)$$

which as it can be seen, are highly non-linear even for the unperturbed problem and thus, they are not appropriate for their direct use of the Koopman operator. To solve this, Ref. [51] proposed to perform a time regularization defined by:

$$\frac{d\theta}{dt} = \frac{p_\theta}{r^2}. \quad (19)$$

where,

$$p_\theta = \sqrt{p_\varphi^2 + \frac{p_\lambda^2}{\cos^2(\varphi)}}, \quad (20)$$

is the angular momentum of the orbit, followed by a set of variable transformations defined by:

$$\begin{aligned} \alpha &= \frac{p_\theta}{r} - \frac{\mu}{p_\theta} = r\sqrt{\dot{\varphi}^2 + \cos^2(\varphi)\dot{\lambda}^2} - \frac{\mu}{r^2\sqrt{\dot{\varphi}^2 + \cos^2(\varphi)\dot{\lambda}^2}}; \\ p_r &= \dot{r}; \\ s &= \sin(\varphi); \\ \gamma &= \frac{p_\varphi}{p_\theta} \cos(\varphi) = \frac{\dot{\varphi} \cos(\varphi)}{\sqrt{\dot{\varphi}^2 + \cos^2(\varphi)\dot{\lambda}^2}}; \\ I_\theta &= \sqrt{p_\varphi^2 + \frac{p_\lambda^2}{\cos^2(\varphi)}} = \frac{1}{r^2\sqrt{\dot{\varphi}^2 + \cos^2(\varphi)\dot{\lambda}^2}}; \\ \beta &= \lambda - \arcsin\left(\tan(\varphi)\sqrt{\frac{p_\lambda^2}{p_\theta^2 - p_\lambda^2}}\right) \\ &= \lambda - \arcsin\left(\tan(\varphi)\dot{\lambda}\sqrt{\frac{\cos^4(\varphi)}{\dot{\varphi}^2 + \cos^2(\varphi)\dot{\lambda}^2 - \cos^4(\varphi)\dot{\lambda}^2}}\right); \\ \xi &= \frac{p_\lambda^2}{p_\theta^2 - p_\lambda^2} = \frac{\cos^4(\varphi)\dot{\lambda}^2}{\dot{\varphi}^2 + \cos^2(\varphi)\dot{\lambda}^2 - \cos^4(\varphi)\dot{\lambda}^2}; \\ p_\lambda &= r^2 \cos^2(\varphi)\dot{\lambda}. \end{aligned} \quad (21)$$

Using this expanded set of orbital elements, the system of differential equa-

tions from Eq. (27) transforms into [51]:

$$\begin{aligned}
 \frac{d\alpha}{d\theta} &= -p_r - \sum_{n=2}^m \mu J_n R_{\oplus}^n \frac{\partial P_n(s)}{\partial s} \gamma I_{\theta}^{n+1} (\alpha + \mu I_{\theta})^{n-1} (\alpha + 2\mu I_{\theta}); \\
 \frac{dp_r}{d\theta} &= \alpha + \sum_{n=2}^m (n+1) \mu J_n R_{\oplus}^n P_n(s) I_{\theta}^{n+1} (\alpha + \mu I_{\theta})^n; \\
 \frac{ds}{d\theta} &= \gamma; \\
 \frac{d\gamma}{d\theta} &= -s - \sum_{n=2}^m \mu J_n R_{\oplus}^n \frac{\partial P_n(s)}{\partial s} p_{\lambda}^2 I_{\theta}^{n+3} (\alpha + \mu I_{\theta})^{n-1}; \\
 \frac{dI_{\theta}}{d\theta} &= \sum_{n=2}^m \mu J_n R_{\oplus}^n \frac{\partial P_n(s)}{\partial s} \gamma I_{\theta}^{n+2} (\alpha + \mu I_{\theta})^{n-1}; \\
 \frac{d\beta}{d\theta} &= - \sum_{n=2}^m \mu J_n R_{\oplus}^n \frac{\partial P_n(s)}{\partial s} \frac{1}{p_{\lambda}} s \xi I_{\theta}^n (\alpha + \mu I_{\theta})^{n-1}; \\
 \frac{d\xi}{d\theta} &= \sum_{n=2}^m 2\mu J_n R_{\oplus}^n \frac{\partial P_n(s)}{\partial s} \frac{1}{p_{\lambda}^2} \gamma \xi^2 I_{\theta}^{n-1} (\alpha + \mu I_{\theta})^{n-1}; \\
 \frac{dp_{\lambda}}{d\theta} &= 0.
 \end{aligned} \tag{22}$$

which, as it can be seen, it is completely polynomial for the variables considered, since p_{λ} is a constant of the motion. This property will allow us to perform the direct analytical integration of the inner products defined before following a simple and fast process.

Unfortunately, this set of equations cannot be used directly with the Koopman operator for two reasons. First, we are looking for a Koopman operator matrix that is independent on the initial conditions since this will allow us to apply the Koopman matrix obtained by the Garlekin method to any orbit. This means that we have to include p_{λ} as a variable in the equations, making the system from Eq. (22) not linear any more under this consideration. Second, when using the Garlekin method we are performing a set of inner products of functions in a given range. Therefore, we require that the variables of the system are normalized in order to bound the maximum values as much as possible. In that regard, the variable ξ from the previous formulation has to be transformed since it is not bounded depending on the initial conditions of the orbit.

4 Formulation to study the zonal harmonics problem using the Koopman operator

In this section we introduce a modified set of elements that allows to apply the Koopman operator while obtaining a good performance in the solution.

To that end, the final goal is to find a Koopman matrix that allows to represent the widest range of orbits possible. In that regard, and since the variable β is not well defined for equatorial orbits, the space of solutions will be separated in two regions. The first one covers the general formulation for orbits that are far from the equatorial orbit. In particular, this region covers any orbit whose inclination is larger than 15 degrees. On the other hand, the second region covers the close to equatorial orbits up to inclinations of 20 degrees. That way, no matter the initial conditions of the satellite, its orbit will be able to be studied, having, in addition, an overlap between both regions in case a mission is flying near the boundary between the defined regions. Moreover it is important to note that these regions can be extended even further at a cost of a gradual lost in precision in the solution.

4.1 General formulation

In order to overcome the limitations of the formulation provided in Eq. (22) when using the Koopman operator, we propose the following modified set of variables for the application in the zonal harmonics problem:

$$\begin{aligned}
 \Lambda &= \sqrt{\frac{R_{\oplus}}{\mu}} \left(\frac{p_{\theta}}{r} - \frac{\mu}{p_{\theta}} \right) = \alpha \sqrt{\frac{R_{\oplus}}{\mu}}; \\
 \eta &= p_r \sqrt{\frac{R_{\oplus}}{\mu}}; \\
 s &= \sin(\varphi); \\
 \gamma &= \frac{p_{\varphi}}{p_{\theta}} \cos(\varphi); \\
 \kappa &= \sqrt{\mu R_{\oplus} p_{\varphi}^2 + \frac{\mu R_{\oplus} p_{\lambda}^2}{\cos^2(\varphi)}} = I_{\theta} \sqrt{\mu R_{\oplus}}; \\
 \beta &= \lambda - \arcsin \left(\tan(\varphi) \sqrt{\frac{p_{\lambda}^2}{p_{\theta}^2 - p_{\lambda}^2}} \right); \\
 \chi &= \frac{p_{\lambda}}{p_{\theta}} \frac{\left(\mu R_{\oplus} p_{\varphi}^2 + \frac{\mu R_{\oplus} p_{\lambda}^2}{\cos^2(\varphi)} \right)^{3/2}}{\sin^2(\varphi) + \frac{p_{\lambda}^2}{p_{\theta}^2} \cos^2(\varphi)} = p_{\lambda} I_{\theta}^4 \frac{(\mu R_{\oplus})^{3/2}}{s^2 + \gamma^2}; \\
 \rho &= \frac{p_{\lambda}}{p_{\theta}} = p_{\lambda} I_{\theta}. \tag{23}
 \end{aligned}$$

Note that in this set of equations, we have normalized several of the original orbital elements making them non-dimensional, and substituted the variable ξ for the element χ which behaves much better than the original variable due to the fact that its value is more constrained for a wide variety of orbits. It is also important to remark that χ is a first integral of the unperturbed problem as in the case of the elements κ , β , and ρ .

When dealing with the general zonal harmonics problem around an oblate celestial body, the derivatives of this new set of orbital elements are:

$$\begin{aligned}
 \frac{d\Lambda}{d\theta} &= -\eta - \sum_{n=2}^m J_n \frac{\partial P_n(s)}{\partial s} \gamma \kappa^{n+1} (\Lambda + \kappa)^{n-1} (\Lambda + 2\kappa); \\
 \frac{d\eta}{d\theta} &= \Lambda + \sum_{n=2}^m (n+1) J_n P_n(s) \kappa^{n+1} (\Lambda + \kappa)^n; \\
 \frac{ds}{d\theta} &= \gamma; \\
 \frac{d\gamma}{d\theta} &= -s - \sum_{n=2}^m J_n \frac{\partial P_n(s)}{\partial s} \rho^2 \kappa^{n+1} (\Lambda + \kappa)^{n-1}; \\
 \frac{d\kappa}{d\theta} &= \sum_{n=2}^m J_n \frac{\partial P_n(s)}{\partial s} \gamma \kappa^{n+2} (\Lambda + \kappa)^{n-1}; \\
 \frac{d\beta}{d\theta} &= -\sum_{n=2}^m J_n \frac{\partial P_n(s)}{\partial s} s \chi \kappa^{n-2} (\Lambda + \kappa)^{n-1}; \\
 \frac{d\chi}{d\theta} &= \sum_{n=2}^m 4J_n \frac{\partial P_n(s)}{\partial s} \gamma \chi \kappa^{n+1} (\Lambda + \kappa)^{n-1} \\
 &\quad + \sum_{n=2}^m 2J_n \frac{\partial P_n(s)}{\partial s} \rho \chi^2 \kappa^{n-2} (\Lambda + \kappa)^{n-1} \\
 &= \sum_{n=2}^m 2J_n \frac{\partial P_n(s)}{\partial s} (2\gamma \kappa^3 + \rho \chi) \chi \kappa^{n-2} (\Lambda + \kappa)^{n-1}; \\
 \frac{d\rho}{d\theta} &= \sum_{n=2}^m J_n \frac{\partial P_n(s)}{\partial s} \gamma \rho \kappa^{n+1} (\Lambda + \kappa)^{n-1}. \tag{24}
 \end{aligned}$$

As it can be seen the former system of differential equations is completely polynomial (note also that the derivatives of the Legendre polynomials P_n are also polynomials in s), and, in addition, all the coefficients of the polynomial are either 1 (corresponding to the unperturbed problem), or a multiple of J_n by a rational number (corresponding to each one of the terms from the zonal harmonics).

4.1.1 Transformation between orbital elements

In general, Eq. (23) can be used to transform spherical coordinates to the set of orbital elements proposed. However, the element β requires a special attention in its definition due to the non uniqueness of its definition due the

arcsine function. This problem can be solved easily by defining β as:

$$\beta = \begin{cases} \lambda - \arcsin\left(\tan(\varphi)\sqrt{\frac{p_\lambda^2}{p_\theta^2 - p_\lambda^2}}\right) & \text{if } p_\varphi \geq 0 \\ \lambda + \arcsin\left(\tan(\varphi)\sqrt{\frac{p_\lambda^2}{p_\theta^2 - p_\lambda^2}}\right) + \pi & \text{if } p_\varphi < 0 \end{cases}. \quad (25)$$

which in that case has the same value of the right ascension of the ascending node of the orbit.

For the inverse transformation, i.e., to transform these set of orbital elements to spherical coordinates, we use the orbital element definitions provided by Eqs. (21) and (23), and the geometrical relations that exist between these variables. Particularly, the spherical coordinates can be obtained following this sequence of operations:

$$\begin{aligned} p_\theta &= \frac{\sqrt{\mu R_\oplus}}{\kappa}; \\ r &= \frac{p_\theta}{\Lambda\sqrt{\frac{\mu}{R_\oplus}} + \frac{\mu}{p_\theta}}; \\ p_r &= \sqrt{\frac{\mu}{R_\oplus}}\eta; \\ \varphi &= \arcsin(s); \\ p_\varphi &= \frac{\gamma}{\cos(\varphi)}p_\theta; \\ si &= \sqrt{s^2 + \gamma^2}; \\ u &= \begin{cases} \arcsin\left(\frac{s}{si}\right) & \text{if } p_\varphi \geq 0 \\ \pi - \arcsin\left(\frac{s}{si}\right) & \text{if } p_\varphi < 0 \end{cases}; \\ \lambda &= \begin{cases} \beta \pm \arccos\left(\frac{\cos(u)}{\cos(\varphi)}\right) & \text{if } s \geq 0 \\ \beta \mp \arccos\left(\frac{\cos(u)}{\cos(\varphi)}\right) & \text{if } s < 0 \end{cases}; \\ p_\lambda &= \rho p_\theta; \end{aligned} \quad (26)$$

where si is the sine of the osculating inclination of the orbit, u is the argument of latitude of the orbit at a given time, and \pm and \mp represent the different solutions when considering prograde (upper symbol) or retrograde (lower symbol) orbits.

4.1.2 Particular case for J2

In the cases where only the J_2 perturbation is considered, the Hamiltonian of the system in spherical coordinates is given by:

$$\mathcal{H} = \frac{1}{2} \left(p_r^2 + \frac{p_\varphi^2}{r^2} + \frac{p_\lambda^2}{r^2 \cos^2(\varphi)} \right) - \frac{\mu}{r} + \frac{1}{2} \mu R_\oplus^2 J_2 \frac{1}{r^3} (3 \sin^2(\varphi) - 1), \quad (27)$$

whose associated Hamilton equations are:

$$\begin{aligned} \frac{dr}{dt} &= p_r; \\ \frac{dp_r}{dt} &= -\frac{\mu}{r^2} + \frac{p_\varphi^2}{r^3} + \frac{p_\lambda^2}{r^3 \cos^2(\varphi)} + \frac{3}{2} \mu J_2 R_\oplus^2 \frac{1}{r^4} (3 \sin^2(\varphi) - 1); \\ \frac{d\varphi}{dt} &= \frac{p_\varphi}{r^2}; \\ \frac{dp_\varphi}{dt} &= -\frac{p_\lambda^2 \sin(\varphi)}{r^2 \cos^3(\varphi)} - 3\mu J_2 R_\oplus^2 \frac{1}{r^3} \sin(\varphi) \cos(\varphi); \\ \frac{d\lambda}{dt} &= \frac{p_\lambda}{r^2 \cos^2(\varphi)}; \\ \frac{dp_\lambda}{dt} &= 0. \end{aligned} \quad (28)$$

Then, if we perform the time regularization, the expansion of the configuration space and the variable transformation described for the zonal problem we obtain the following system of equations:

$$\begin{aligned} \frac{d\Lambda}{d\theta} &= -\eta - 3J_2 s \gamma \kappa^3 (\Lambda + \kappa) (\Lambda + 2\kappa); \\ \frac{d\eta}{d\theta} &= \Lambda + \frac{3}{2} J_2 \kappa^3 (\Lambda + \kappa)^2 (3s^2 - 1); \\ \frac{ds}{d\theta} &= \gamma; \\ \frac{d\gamma}{d\theta} &= -s - 3J_2 s \rho^2 \kappa^3 (\Lambda + \kappa); \\ \frac{d\kappa}{d\theta} &= 3J_2 s \gamma \kappa^4 (\Lambda + \kappa); \\ \frac{d\beta}{d\theta} &= -3J_2 s^2 \chi (\Lambda + \kappa); \\ \frac{d\chi}{d\theta} &= 12J_2 s \gamma \chi \kappa^3 (\Lambda + \kappa) + 6J_2 s \rho \chi^2 (\Lambda + \kappa); \\ \frac{d\rho}{d\theta} &= 3J_2 s \gamma \rho \kappa^3 (\Lambda + \kappa). \end{aligned} \quad (29)$$

which is again completely polynomial.

4.2 Close to equatorial orbits

Orbits that are close to the Equator present two difficulties when using the former formulation. First, the variable β is not well defined in a similar way in which the right ascension of the ascending node in keplerian variables is not well defined for equatorial orbits. Second, the value of the variable χ can increase too much for the Garlekin method to properly approximate the variable in the ranges of application. For this reason, we use a different formulation for orbits that are close to equatorial.

We start with the Hamilton equations expressed in spherical coordinates provided by Eq. (18). From this system of differential equations we perform a time regularization, but instead of using θ as the time regularization variable as in the previous case, we use a new independent variable τ defined by:

$$\frac{d\tau}{dt} = \frac{p_\theta}{r^2 \cos^2(\varphi)}, \quad (30)$$

and introduce it in the system of differential equations from Eq. (18) to obtain:

$$\begin{aligned} \frac{dr}{d\tau} &= \frac{p_r}{p_\theta} r^2 \cos^2(\varphi); \\ \frac{dp_r}{d\tau} &= -\frac{\mu}{p_\theta} \cos^2(\varphi) + \frac{1}{r} \frac{p_\varphi^2}{p_\theta} \cos^2(\varphi) + \frac{1}{r} \frac{p_\lambda^2}{p_\theta} \\ &\quad + \sum_{n=2}^m (n+1) \mu J_n P_n(\sin(\varphi)) \frac{R_\oplus^n}{r^n} \frac{1}{p_\theta} \cos^2(\varphi); \\ \frac{d\varphi}{d\tau} &= \frac{p_\varphi}{p_\theta} \cos^2(\varphi); \\ \frac{dp_\varphi}{d\tau} &= -\frac{p_\lambda^2}{p_\theta} \tan(\varphi) - \sum_{n=2}^m \mu J_n \frac{\partial P_n(\sin(\varphi))}{\partial \varphi} \frac{1}{p_\theta} \frac{R_\oplus^n}{r^{n-1}} \cos^2(\varphi); \\ \frac{d\lambda}{d\tau} &= \frac{p_\lambda}{p_\theta}; \\ \frac{dp_\lambda}{d\tau} &= 0. \end{aligned} \quad (31)$$

Similarly to the previous section, we perform the variable transformation for A , η , s , γ , and ρ , and expand the configuration space of the problem with variable κ . In this regard, note that variable χ is not required to represent this region of the space. Following these transformations, the system of

differential equations becomes:

$$\begin{aligned}
 \frac{d\Lambda}{d\tau} &= -\eta(1-s^2) - \sum_{n=2}^m J_n \frac{\partial P_n(s)}{\partial s} \gamma \kappa^{n+1} (\Lambda + \kappa)^{n-1} (\Lambda + 2\kappa) (1-s^2); \\
 \frac{d\eta}{d\tau} &= \Lambda(1-s^2) + \sum_{n=2}^m (n+1) J_n P_n(s) \kappa^{n+1} (\Lambda + \kappa)^n (1-s^2); \\
 \frac{ds}{d\tau} &= \gamma(1-s^2); \\
 \frac{d\gamma}{d\tau} &= -s(1-s^2) - \sum_{n=2}^m J_n \frac{\partial P_n(s)}{\partial s} \rho^2 \kappa^{n+1} (\Lambda + \kappa)^{n-1} (1-s^2); \\
 \frac{d\kappa}{d\tau} &= \sum_{n=2}^m J_n \frac{\partial P_n(s)}{\partial s} \gamma \kappa^{n+2} (\Lambda + \kappa)^{n-1} (1-s^2); \\
 \frac{d\lambda}{d\tau} &= \rho; \\
 \frac{d\rho}{d\tau} &= \sum_{n=2}^m J_n \frac{\partial P_n(s)}{\partial s} \gamma \rho \kappa^{n+1} (\Lambda + \kappa)^{n-1} (1-s^2). \tag{32}
 \end{aligned}$$

Note that this system of differential equations is still polynomial, but contrary to what happens in the previous formulation, the non-perturbed problem is non-linear. This may seem like a limiting factor for the application of the Koopman operator, however, the non-linearities of the unperturbed problem are in fact small when compared with the linear part, making the system nearly linear. This property allows us to directly apply the Koopman operator to this system of differential equations while still obtaining a good performance in the results. Unfortunately, even with these transformations, the solution for the variables s and γ provided by the Koopman operator perform poorly as we increase the inclination of the orbit. Therefore, these orbital elements must be modified to improve the performance. This is done via a normalization of these variables.

Let ψ be a constant value such that $\psi > \sin(i)$ where i is the maximum inclination of the orbits we are interested in. In our case, and since we want to cover all the space of solutions including some overlap, we define $\psi = \sin(20^\circ)$. Note that this value can be reduced to improve performance if we are interested in orbits with lower inclinations. In particular, the closer the value of ψ is to $\sin(i)$ of the orbit, the better is the performance obtained as long as $\psi > \sin(i)$. On the other hand, it is not convenient to increase the value of ψ over 1 since that will make the differential equations more non-linear, reducing in consequence the performance of the solution.

Based on this constant ψ we define two transformations:

$$\begin{aligned}\sigma &= \frac{s}{\psi}; \\ \Gamma &= \frac{\gamma}{\psi};\end{aligned}\tag{33}$$

and introduce them into the set of differential equations to obtain:

$$\begin{aligned}\frac{d\Lambda}{d\tau} &= -\eta(1 - \psi^2\sigma^2) \\ &\quad - \sum_{n=2}^m \psi J_n \frac{\partial P_n(\psi\sigma)}{\partial(\psi\sigma)} \Gamma \kappa^{n+1} (\Lambda + \kappa)^{n-1} (\Lambda + 2\kappa) (1 - \psi^2\sigma^2); \\ \frac{d\eta}{d\tau} &= \Lambda(1 - \psi^2\sigma^2) + \sum_{n=2}^m (n+1) J_n P_n(\psi\sigma) \kappa^{n+1} (\Lambda + \kappa)^n (1 - \psi^2\sigma^2); \\ \frac{d\sigma}{d\tau} &= \Gamma(1 - \psi^2\sigma^2); \\ \frac{d\Gamma}{d\tau} &= -\sigma(1 - \psi^2\sigma^2) - \sum_{n=2}^m \frac{1}{\psi} J_n \frac{\partial P_n(\psi\sigma)}{\partial(\psi\sigma)} \rho^2 \kappa^{n+1} (\Lambda + \kappa)^{n-1} (1 - \psi^2\sigma^2); \\ \frac{d\kappa}{d\tau} &= \sum_{n=2}^m \psi J_n \frac{\partial P_n(\psi\sigma)}{\partial(\psi\sigma)} \Gamma \kappa^{n+2} (\Lambda + \kappa)^{n-1} (1 - \psi^2\sigma^2); \\ \frac{d\lambda}{d\tau} &= \rho; \\ \frac{d\rho}{d\tau} &= \sum_{n=2}^m \psi J_n \frac{\partial P_n(\psi\sigma)}{\partial(\psi\sigma)} \Gamma \rho \kappa^{n+1} (\Lambda + \kappa)^{n-1} (1 - \psi^2\sigma^2);\end{aligned}\tag{34}$$

which can finally be applied directly to the Koopman operator formulation for any orbit whose inclination is smaller than $\arcsin(\psi)$. Note also that now the coefficients of the polynomials of the unperturbed problem that are non-linear (ψ^2) are small compared to the linear term. In fact, the Koopman operator treats these terms as another perturbation of the linear system, which is why it is possible to apply this non-linear formulation.

4.2.1 Particular case for J_2

As in the zonal case, we include the particular case of the J_2 term of the gravitational potential for completeness and due to the fact that it is the most important term for orbiting satellites around the Earth. In that regard the system of differential equations when taking into account just the

oblateness of the Earth (J_2 term of the Earth gravitational potential) is:

$$\begin{aligned}
 \frac{d\Lambda}{d\tau} &= -\eta(1 - \psi^2\sigma^2) - 3\psi^2 J_2 \sigma \Gamma \kappa^3 (\Lambda + \kappa) (\Lambda + 2\kappa) (1 - \psi^2\sigma^2); \\
 \frac{d\eta}{d\tau} &= \Lambda(1 - \psi^2\sigma^2) + \frac{3}{2} J_2 \kappa^3 (\Lambda + \kappa)^2 (3\psi^2\sigma^2 - 1) (1 - \psi^2\sigma^2); \\
 \frac{d\sigma}{d\tau} &= \Gamma(1 - \psi^2\sigma^2); \\
 \frac{d\Gamma}{d\tau} &= -\sigma(1 - \psi^2\sigma^2) - 3J_2 \sigma \rho^2 \kappa^3 (\Lambda + \kappa) (1 - \psi^2\sigma^2); \\
 \frac{d\kappa}{d\tau} &= 3\psi^2 J_2 \sigma \Gamma \kappa^4 (\Lambda + \kappa) (1 - \psi^2\sigma^2); \\
 \frac{d\lambda}{d\tau} &= \rho; \\
 \frac{d\rho}{d\tau} &= 3\psi^2 J_n \sigma \Gamma \rho \kappa^3 (\Lambda + \kappa) (1 - \psi^2\sigma^2).
 \end{aligned} \tag{35}$$

5 Examples of application

In this section we show the result of applying the methodology described in this work to different orbits. In particular, we show three cases of application: a near circular sun-synchronous orbit, a Molniya orbit, a hyperbolic orbit, and a near-equatorial orbit. This will allow us to show the performance of the formulation for some characteristic orbits. In addition, we also include the results for different orders of basis functions to show how the Koopman operator methodology performs and converges to the solution of the system of differential equations. In that regard, it is important to note that the set of differential equations provided by Eqs. (29) and (35) are based on polynomials in odd powers. This means that only the basis functions containing terms in an odd power in the polynomial contribute to the representation of the differential equation. For that reason, in the examples provided we focus on the use of basis function with a maximum order that is odd.

The examples provided focus on LEO orbits due to the fact that the zonal harmonics perturbation is larger in this region. Therefore, a much better performance should be expected as the altitude of the orbits increases. Moreover, all of the examples included are compared to a numerical integration of the system using a Runge-Kutta scheme of order 4-5 to show the performance of the methodology for different scenarios.

5.1 Sun-synchronous orbit

For this example, a sun-synchronous frozen Earth observation orbit is selected with the initial orbital conditions: semi-major axis $a = 7077.722$ km, eccentricity $e = 0.001043$, inclination $i = 98.186$ deg, argument of perigee

$\omega = 90.0$ deg, right ascension of the ascending node $\Omega = 0.0$ deg and true anomaly $\nu = 0.0$ deg. Figure 1 (left) shows the evolution of the radial distance (r), the latitude (φ), and the longitude (λ) of the orbit as a function of the independent variable θ (defined as the time regularization variable in Eq. (19)). Moreover, Figure 1 (right) shows the comparison of the Koopman operator solution using basis functions of order 7 with the numerical integration of the equations. From these results, it can be observed that the error of this solution is in the order of magnitude of the meters in the position of the satellite (both taking into account both the radial distance and the angles latitude and longitude of the orbit).

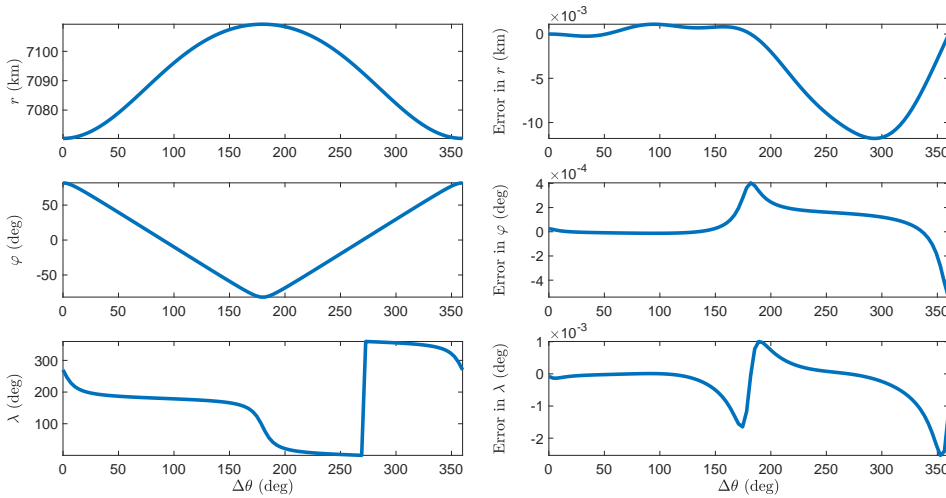


Figure 1: 7th order solution and error in $\{r, \varphi, \lambda\}$ for a frozen sun-synchronous orbit.

The result from Figure 1 can be improved by increasing the order of the basis functions used in the Koopman operator approach. In that regard, Figure 2 shows the errors of the solution for the 9th (left) and 11th (right) order basis function solutions when compared to the numerical integration. As it can be seen, the maximum error is reduced to a couple of meters and less than 0.32 meters respectively. This shows that the solution is getting closer to the real evolution of the system by increasing the order of the basis functions used to represent the system of differential equations.

Moreover, we can also study the long term evolution of these solutions. To that end, Figure 3 shows the error for a propagation of 100 orbital revolutions when using a set of basis functions of order 7th (left) and 9th (right). As it can be observed, the error of the solution quickly increases with time. Nevertheless, the error reduces with the increase on the order of the basis functions. Thus, it is possible to improve the long term performance of the methodology by further increasing the order of the basis functions used.

Additionally, it is also possible to study the spectral structure of the

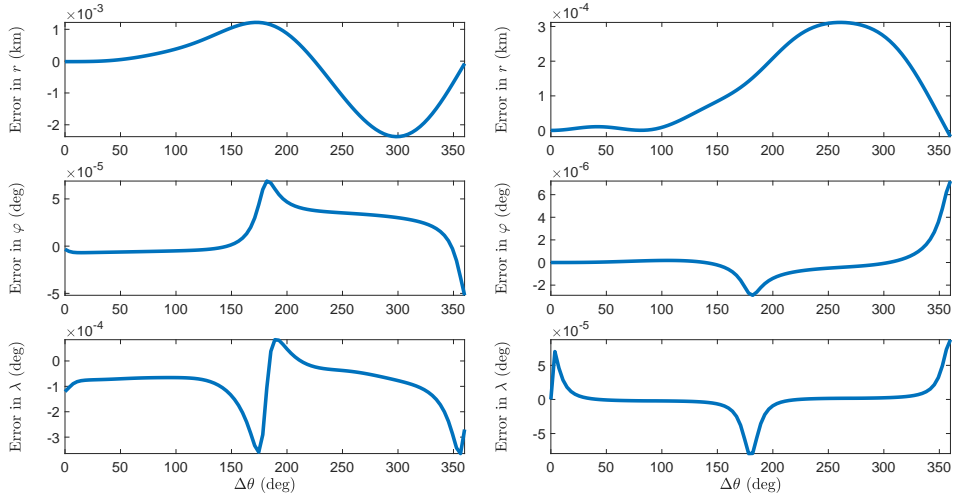


Figure 2: 9th and 11th order solution error in $\{r, \varphi, \lambda\}$ for a frozen sun-synchronous orbit.

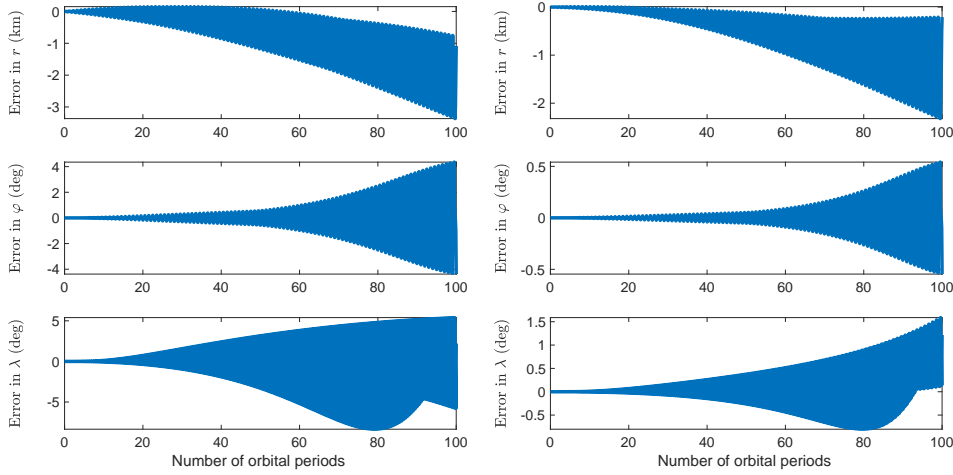


Figure 3: 7th and 9th order solution error for a long term propagation in $\{r, \varphi, \lambda\}$ for a frozen sun-synchronous orbit.

solution. To that end, Figure 4 shows the distribution of eigenvalues of the system when using a set of basis functions of order 7 (left) and 9 (right) respectively. In that regard, it is important to note that, since the Koopman matrix is independent of the initial conditions of the orbit, these eigenvalues are valid for any orbit that the dynamical system provided by Eq. (29) is able to represent. As it can be seen in the figure, the maximum values of the frequencies are 7 and 9 respectively. In that respect, we know that the eigenvalues of the unperturbed problem using the system from Eq. (29) are $\pm i$ and 0. However, since the basis functions are built as a combination of

the initial set of variables, the maximum frequency of the system increases with the order of the basis functions used. Particularly, let ϕ_1 and ϕ_2 be two eigenfunctions of the Koopman matrix with associated eigenvalues E_1 and E_2 respectively, therefore:

$$\begin{aligned}\frac{d\phi_1}{dt} &= E_1\phi_1; \\ \frac{d\phi_2}{dt} &= E_2\phi_2.\end{aligned}\tag{36}$$

Then, we can define a third function g as the multiplication of the first two, that is: $g = \phi_1\phi_2$. If we introduce it in the dynamical system we obtain:

$$\frac{dg}{dt} = \frac{d\phi_1}{dt}\phi_2 + \phi_1\frac{d\phi_2}{dt} = E_1\phi_1\phi_2 + E_2\phi_1\phi_2 = (E_1 + E_2)\phi_1\phi_2 = (E_1 + E_2)g,\tag{37}$$

which means that g is also an eigenfunction of the system with associated eigenvalue $E_1 + E_2$. This is the reason why the maximum frequency that we observe in Figure 4 matches the maximum order of the basis functions used. On the other hand, Figure 4 also shows that there are some eigenvalues with real part different to zero. These eigenvalues are generated by the multiple combinations of the basis functions related with the secular variation of the right ascension of the ascending node (represented by variable β) with the rest of variables involved in the problem.

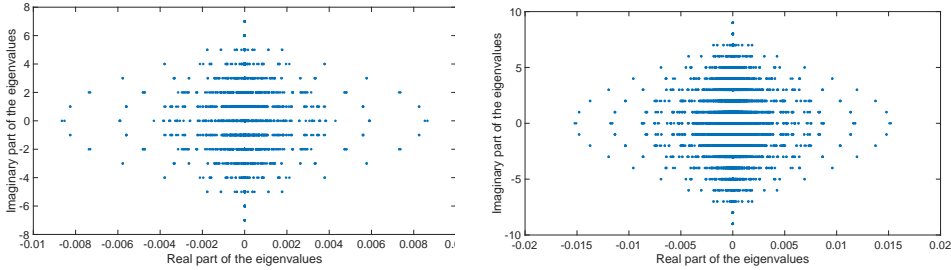
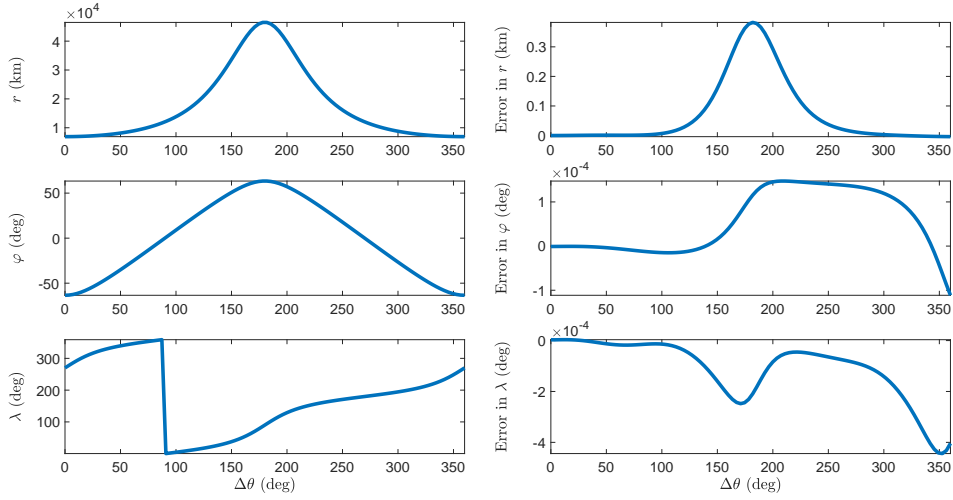
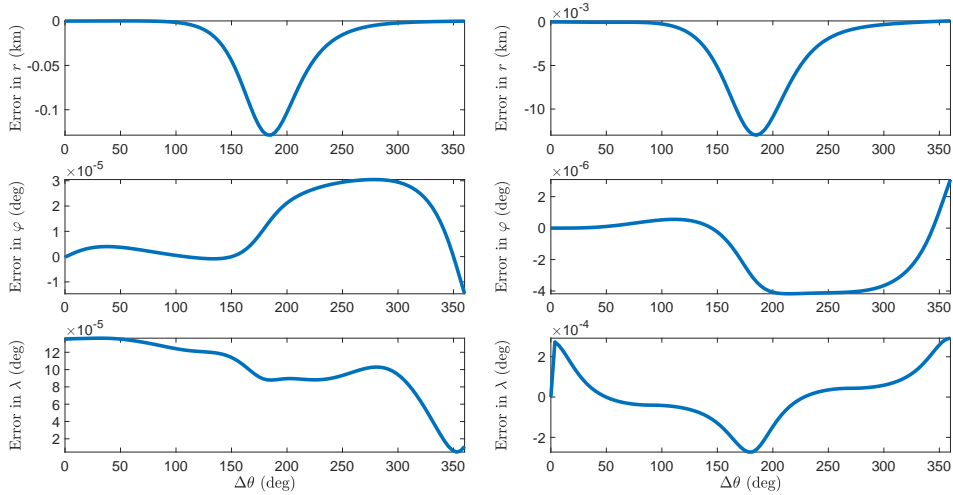


Figure 4: 7th and 9th order eigenvalues for the general formulation case.

5.2 Molniya orbit

We select a typical molniya orbit as an example of application to eccentric orbits. Particularly, we set the initial conditions for the propagation to: $a = 26600.0$ km, $e = 0.74$, $i = 63.435$ deg, $\omega = 270.0$ deg, $\Omega = 0.0$ deg and $\nu = 0.0$ deg. Figure 5 shows the results for the evolution of $\{r, \varphi, \lambda\}$ and their error when using a set of basis functions of order 7. As it can be seen, the maximum error observed (less than 400 m) is now bigger than in the case of the sun-synchronous orbit. Nevertheless, this is consistent with the results from the previous example having a relative error in the order of magnitude of 10^{-5} .


 Figure 5: 7th order solution and error in $\{r, \varphi, \lambda\}$ for a molniya orbit.

 Figure 6: 9th and 11th order solution error in $\{r, \varphi, \lambda\}$ for a molniya orbit.

In addition, Figure 6 shows the error on the position when using a set of basis functions of order 9 (left) and 11 (right) respectively. As it can be seen, the error in this case is of 10s of meters. This shows that the formulation and methodology presented can be applied to very eccentric orbits while obtaining a good accuracy.

5.3 Hyperbolic orbit

For the example of hyperbolic orbit, we select the following initial conditions: $a = -35000.0$ km, $e = 1.2$, $i = 50.0$ deg, $\omega = 0.0$ deg, $\Omega = 0.0$ deg and $\nu = 0.0$ deg. Figure 7 shows the results of the propagation and associated

errors for a Koopman solution using basis functions of order 7, while Figure 8 does the same for orders 9 (left) and 11 (right). Note that in this case, the propagation has been extended just to $\theta = 120^\circ$ in order to prevent the variables to become extremely large. Nevertheless, it can be seen from the figures that the precision of the solution is also maintained in this case, having a maximum error on the order of magnitude of meters even for the hyperbolic case.

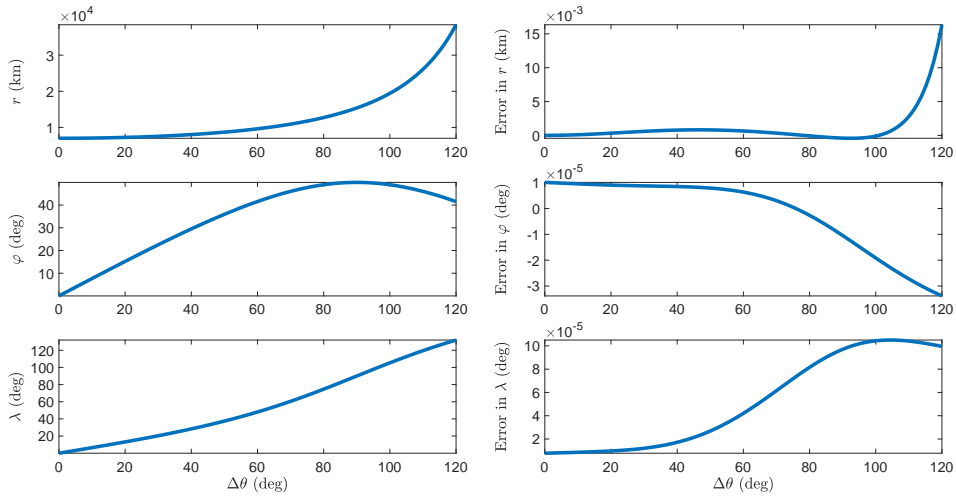


Figure 7: 7th order solution and error in $\{r, \varphi, \lambda\}$ for a hyperbolic orbit.

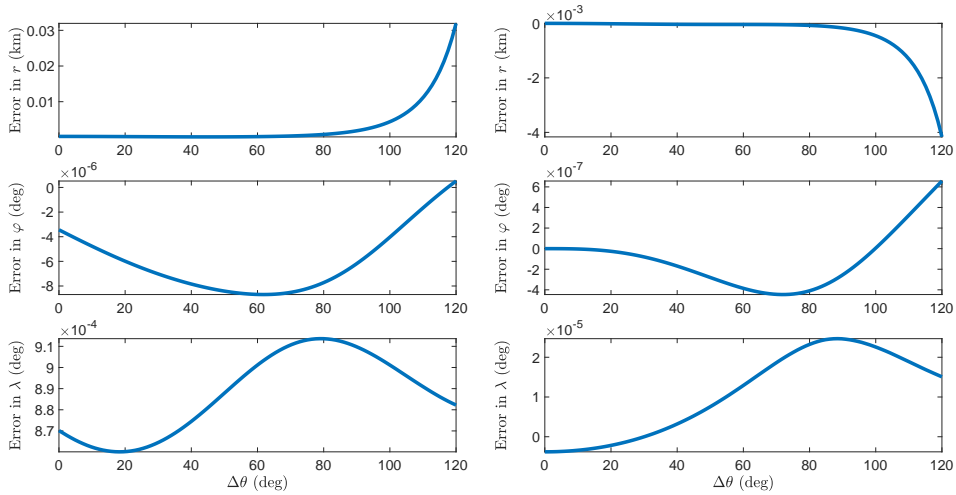


Figure 8: 9th and 11th order solution error in $\{r, \varphi, \lambda\}$ for a hyperbolic orbit.

Note that sometimes applying a set of higher order basis functions produces a slightly decrease in accuracy in the methodology, especially in the longitude of the orbit. This can be seen, for instance, in the errors in lati-

tude of Figure 2 for the cases of 9th and 11th orders, or in error in latitude for this hyperbolic example for orders 7 and 9 (Figures 7 and 8). However, if the order of the basis functions is further increased, this anomalous behavior disappears. An example of that can be seen in Figure 8 in the latitude of the solution for basis functions of orders 9 and 11. This happens due to numerical errors appearing during the eigendecomposition of the Koopman matrix and subsequent inversion of the matrix of eigenvectors.

5.4 Near equatorial orbit

This final example is included to show the performance of the formulation for close to equatorial orbits. Particularly, the initial conditions selected for this examples are: $a = 7192.15$ km, $e = 0$, $i = 5$ deg, $\omega = -90$ deg, $\Omega = 0.0$ deg and $\nu = 180.0$ deg. As in the previous examples, Figures 9 and 10 show the evolution of the position and the errors for the Koopman operator methodology when using basis functions of orders 7, 9 and 11 respectively. As it can be seen from these figures, the errors are of the same order of magnitude as the ones seen in the previous examples, which shows the performance of this alternative formulation when applied to near-equatorial orbits

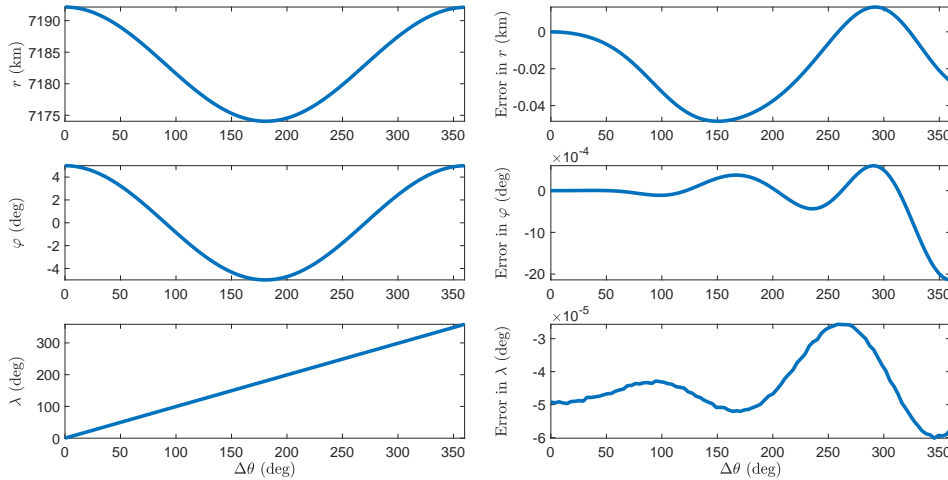


Figure 9: 7th order solution and error in $\{r, \varphi, \lambda\}$ for a 5 deg inclination orbit.

Additionally, and since the Koopman matrix is different from the one used in the previous examples (due to the fact that we are using a slightly different formulation), it is interesting to study the difference in the distribution of eigenvalues of this system. In that regard, Figure 11 shows a map containing all the eigenvalues when using eigenfunctions of order 7 and 9 respectively. As it can be seen, the distribution is different from Figure 4, particularly the real parts of the eigenvalues. This is due to the different

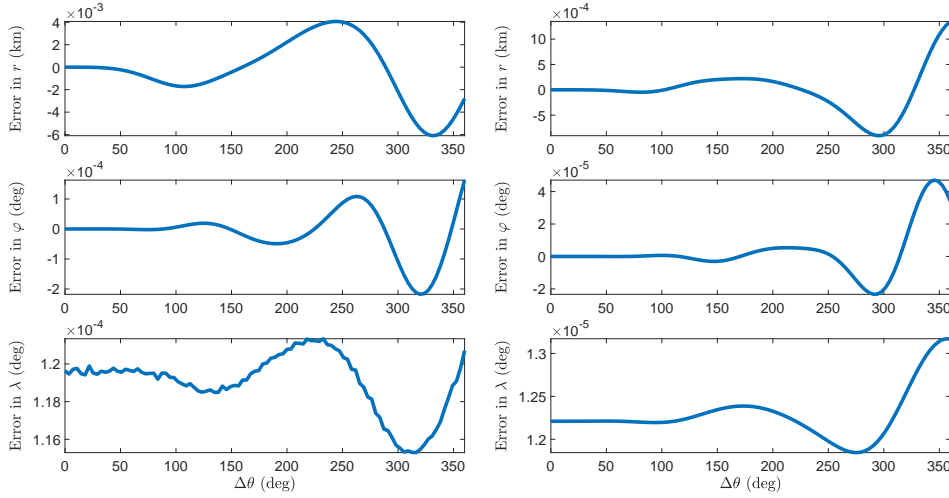


Figure 10: 9th and 11th order solution error in $\{r, \varphi, \lambda\}$ for a 5 deg inclination orbit.

nature of both formulations. In the general case, we have as an orbital element a variable whose secular value matches the one of the right ascension of the ascending node. However, in the close to equatorial case, that variable was substituted by another whose derivative was linear with the ratio p_λ/p_θ . Additionally, the close to equatorial formulation does not require the additional variable χ which also generates a large number of these eigenvalues with non-zero real part. This shows the importance of selecting an adequate formulation for the use alongside with the Koopman operator since it greatly depends on the eigendecomposition of the system.

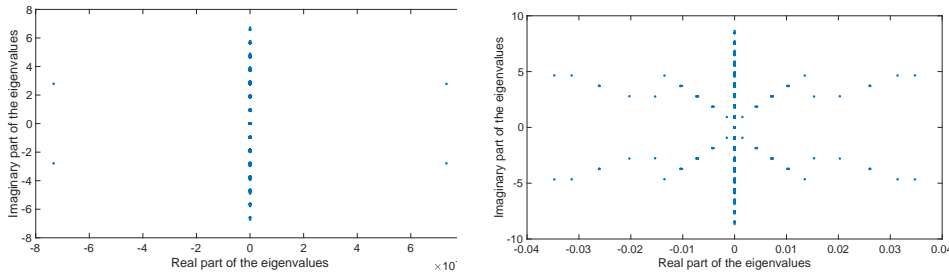


Figure 11: 7th and 9th order eigenvalues for the close to equatorial formulation.

6 Conclusion

This manuscript focuses on the application of the Koopman operator theory to the zonal harmonics problem of a satellite orbiting an oblate celestial

body. This represents the first attempt of using operator theory in this important problem in astrodynamics. To that end, this work presents a summary of the Koopman operator theory and how to apply it effectively into the zonal harmonics problem using a set of modified orbital elements that allow to represent any kind of orbit, including, circular, elliptic, parabolic and hyperbolic orbits.

The Koopman operator methodology allows us to obtain in an automated process any order of the solution by an extension of the set of basis functions used to represent the solution. Therefore, this methodology allows the error to be adjusted to any precision required. In that regard, four examples of application are shown in this manuscript, showing the performance results of this methodology to very characteristic orbits in celestial mechanics, including a sun-synchronous frozen orbit, a molniya orbit, a hyperbolic orbit and a close to equatorial orbit. These examples show that it is possible to obtain relative errors of 10^{-5} when using this methodology for the different cases of application. Similar performance have been observed for other orbits in the same range of altitudes. In that regard, it is important to note that as the altitude of the orbit increases, the perturbation produced by the zonal harmonic terms of the gravitational potential is also reduced, and thus, the performance of the methodology also improves accordingly. For instance, for a geo-synchronous orbit, less than 1 cm errors were observed for the same order of basis functions considered in this work.

Compared to other methodologies that focus on the zonal harmonics problem, the Koopman operator directly provides the osculating variation of all the variables involved in the problem, as opposed to other approaches where it is required to define some intermediaries or the transformation of orbital elements. Additionally, the Koopman operator allows us to handle automatically any order of the zonal harmonics of the gravitational potential, not requiring to modify the methodology in any way to obtain the solution. Another interesting result of the Koopman operator is that the methodology provides the spectral behavior of the system, which can be used to study some properties of the problem. Finally, since the Koopman matrix is obtained as part of the methodology, this matrix represents the best linear approximation of the problem with the set of basis functions and variable ranges defined. This can be used for other applications, including control schemes.

Acknowledgements

The authors wish to thank Daniel Jang at Massachusetts Institute of Technology for his help in reviewing and improving the use of English in this manuscript.

References

- [1] M. Irigoyen and C. Simo. “Non integrability of the J₂ problem”. In: *Celestial Mechanics and Dynamical Astronomy* 55.3 (1993), pp. 281–287. DOI: 10.1007/BF00692515.
- [2] A. Celletti and P. Negrini. “Non-integrability of the problem of motion around an oblate planet”. In: *Celestial Mechanics and Dynamical Astronomy* 61.3 (1995), pp. 253–260. DOI: 10.1007/BF00051896.
- [3] D. Brouwer. “Solution of the problem of artificial satellite theory without drag”. In: *The Astronomical Journal* 64 (1959), pp. 378–397.
- [4] Y. Kozai. “The motion of a close earth satellite”. In: *The Astronomical Journal* 64 (1959), p. 367.
- [5] Y. Kozai. “Second-order solution of artificial satellite theory without air drag”. In: *The Astronomical Journal* 67 (1962), p. 446.
- [6] A. Deprit. “Canonical transformations depending on a small parameter”. In: *Celestial Mechanics* 1.1 (1969), pp. 12–30. DOI: 10.1007/BF01230629.
- [7] J. Liu. “Satellite motion about an oblate Earth”. In: *AIAA Journal* 12.11 (1974), pp. 1511–1516. DOI: 10.2514/3.49537.
- [8] A. Deprit. “The elimination of the parallax in satellite theory”. In: *Celestial Mechanics* 24.2 (1981), pp. 111–153. DOI: 10.1007/BF01229192.
- [9] A. Deprit. “The main problem in the theory of artificial satellites to order four”. In: *Journal of Guidance and Control* 4.2 (1981), pp. 201–206. DOI: 10.2514/3.56072.
- [10] S. Coffey and A. Deprit. “Third-order solution to the main problem in satellite theory”. In: *Journal of Guidance, Control, and Dynamics* 5.4 (1982), pp. 366–371. DOI: 10.2514/3.56183.
- [11] K. T. Alfriend and S. L. Coffey. “Elimination of the perigee in the satellite problem”. In: *Celestial Mechanics* 32 (1984), 163–172. DOI: 10.1007/BF01231123.
- [12] A. Kamel and T. Duhamel. “A second-order solution of the main problem of artificial satellites using multiple scales”. In: *Journal of Guidance, Control, and Dynamics* 8.1 (1985), pp. 125–133. DOI: 10.2514/3.19944.
- [13] Y. Hashida and P. L. Palmer. “Epicyclic motion of satellites about an oblate planet”. In: *Journal of Guidance, Control, and Dynamics* 24.3 (2001), pp. 586–596. DOI: 10.2514/2.4750.
- [14] I. M. Ross. “Linearized dynamic equations for spacecraft subject to j perturbations”. In: *Journal of guidance, control, and dynamics* 26.4 (2003), pp. 657–659. DOI: 10.2514/2.5095.

- [15] M. Humi. “J2 Effect in Cylindrical Coordinates”. In: *Journal of guidance, control, and dynamics* 30.1 (2007), pp. 263–266. DOI: 10.2514/1.22517.
- [16] R. Broucke. “Stability of periodic orbits in the elliptic, restricted three-body problem”. In: *AIAA journal* 7.6 (1969), pp. 1003–1009. DOI: 10.2514/3.5267.
- [17] C. R. McInnes. “Dynamics, stability, and control of displaced non-Keplerian orbits”. In: *Journal of Guidance, Control, and Dynamics* 21.5 (1998), pp. 799–805. DOI: 10.2514/2.4309.
- [18] D. Scheeres, M. Guman, and B. Villac. “Stability analysis of planetary satellite orbiters: application to the Europa orbiter”. In: *Journal of Guidance, Control, and Dynamics* 24.4 (2001), pp. 778–787. DOI: 10.2514/2.4778.
- [19] D. Arnas, D. Casanova, and E. Tresaco. “Relative and Absolute Station-Keeping for Two-Dimensional–Lattice Flower Constellations”. In: *Journal of Guidance, Control, and Dynamics* 39.11 (2016), pp. 2602–2604. DOI: 10.2514/1.G000358.
- [20] C. N. McGrath and M. Macdonald. “General perturbation method for satellite constellation reconfiguration using low-thrust maneuvers”. In: *Journal of Guidance, Control, and Dynamics* 42.8 (2019), pp. 1676–1692. DOI: 10.2514/1.G003739.
- [21] D. Arnas and D. Casanova. “Nominal definition of satellite constellations under the Earth gravitational potential”. In: *Celestial Mechanics and Dynamical Astronomy* 132 (2020), pp. 1–20. DOI: 10.1007/s10569-020-09958-4.
- [22] J.-F. Hamel and J. de Lafontaine. “Linearized dynamics of formation flying spacecraft on a J2-perturbed elliptical orbit”. In: *Journal of Guidance, Control, and Dynamics* 30.6 (2007), pp. 1649–1658. DOI: 10.2514/1.29438.
- [23] S. R. Vadali. “Model for linearized satellite relative motion about a J2-perturbed mean circular orbit”. In: *Journal of guidance, control, and dynamics* 32.5 (2009), pp. 1687–1691. DOI: 10.2514/1.42955.
- [24] D. Arnas, P. Jurado, I. Barat, B. Duesmann, and R. Bock. “FLEX: A Parametric Study of Its Tandem Formation With Sentinel-3”. In: *IEEE Journal of Selected Topics in Applied Earth Observations and Remote Sensing* 12.7 (2019), pp. 2447–2452. DOI: 10.1109/JSTARS.2019.2896196.
- [25] D. Arnas. “Linearized model for satellite station-keeping and tandem formations under the effects of atmospheric drag”. In: *Acta Astronautica* 178 (2021), pp. 835–845. DOI: 10.1016/j.actaastro.2020.10.035.

- [26] R. Lyddane. “Small eccentricities or inclinations in the Brouwer theory of the artificial satellite”. In: *The Astronomical Journal* 68 (1963), p. 555. DOI: 10.1086/109179.
- [27] C. Cohen and R. Lyddane. “Radius of convergence of Lie series for some elliptic elements”. In: *Celestial Mechanics* 25.3 (1981), pp. 221–234. DOI: 10.1007/BF01228961.
- [28] S. L. Coffey, A. Deprit, and B. R. Miller. “The critical inclination in artificial satellite theory”. In: *Celestial Mechanics* 39.4 (1986), pp. 365–406. DOI: 10.1007/BF01230483.
- [29] A. A. Kamel. “Expansion formulae in canonical transformations depending on a small parameter”. In: *Celestial Mechanics* 1.2 (1969), pp. 190–199. DOI: 10.1007/BF01228838.
- [30] A. A. Kamel. “Perturbation method in the theory of nonlinear oscillations”. In: *Celestial Mechanics* 3.1 (1970), pp. 90–106. DOI: 10.1007/BF01230435.
- [31] A. Deprit and A. Rom. “The main problem of artificial satellite theory for small and moderate eccentricities”. In: *Celestial Mechanics* 2.2 (1970), pp. 166–206. DOI: 10.1007/BF01229494.
- [32] A. Deprit. “Delaunay normalisations”. In: *Celestial Mechanics* 26.1 (1982), pp. 9–21. DOI: 10.1007/BF01233178.
- [33] R. Cid, S. Ferrer, and M. Sein-Echaluce. “On the radial intermediaries and the time transformation in satellite theory”. In: *Celestial Mechanics* 38.2 (1986), pp. 191–205. DOI: 10.1007/BF01230431.
- [34] A. Abad, J. San-Juan, and A. Gavín. “Short term evolution of artificial satellites”. In: *Celestial Mechanics and Dynamical Astronomy* 79.4 (2001), pp. 277–296. DOI: 10.1023/A:1017540603450.
- [35] A. Abad, M. Calvo, and A. Elipe. “Integration of Deprit’s radial intermediary”. In: *Acta Astronautica* 173 (2020), pp. 19–21. DOI: 10.1016/j.actaastro.2020.03.039.
- [36] B. Mahajan, S. R. Vadali, and K. T. Alfriend. “Exact Delaunay normalization of the perturbed Keplerian Hamiltonian with tesseral harmonics”. In: *Celestial Mechanics and Dynamical Astronomy* 130.3 (2018), p. 25. DOI: 10.1007/s10569-018-9818-8.
- [37] M. Lara. “Solution to the main problem of the artificial satellite by reverse normalization”. In: *Nonlinear Dynamics* 101.2 (2020), pp. 1501–1524. DOI: 10.1007/s11071-020-05857-3.
- [38] J. B. Conway. *A course in functional analysis*. Vol. 96. Springer, 2019. ISBN: 978-1-4757-3830-8. DOI: 10.1007/978-1-4757-3828-5.
- [39] K. Kowalski and W.-h. Steeb. *Nonlinear dynamical systems and Carleman linearization*. World Scientific, 1991. ISBN: 978-9810205874.

- [40] I. Prigogine. *Non-equilibrium statistical mechanics*. Dover Publications, 1962. ISBN: 978-0486815558.
- [41] A. Naylor and G. Sell. *Linear Operator Theory in Engineering and Science*. Applied Mathematical Sciences. Springer, 2000. ISBN: 9780387950013.
- [42] M. O. Williams, I. G. Kevrekidis, and C. W. Rowley. “A data-driven approximation of the koopman operator: Extending dynamic mode decomposition”. In: *Journal of Nonlinear Science* 25.6 (2015), pp. 1307–1346. DOI: 10.1007/s00332-015-9258-5.
- [43] I. Mezić. “Analysis of fluid flows via spectral properties of the Koopman operator”. In: *Annual Review of Fluid Mechanics* 45 (2013), pp. 357–378. DOI: 10.1146/annurev-fluid-011212-140652.
- [44] S. L. Brunton, B. W. Brunton, J. L. Proctor, and J. N. Kutz. “Koopman invariant subspaces and finite linear representations of nonlinear dynamical systems for control”. In: *PloS one* 11.2 (2016), e0150171. DOI: 10.1371/journal.pone.0150171.
- [45] A. Surana and A. Banaszuk. “Linear observer synthesis for nonlinear systems using Koopman operator framework”. In: *IFAC-PapersOnLine* 49.18 (2016), pp. 716–723. DOI: 10.1016/j.ifacol.2016.10.250.
- [46] A. Surana. “Koopman operator based observer synthesis for control-affine nonlinear systems”. In: *Decision and Control (CDC), 2016 IEEE 55th Conference on*. IEEE. 2016, pp. 6492–6499. DOI: 10.1109/CDC.2016.7799268.
- [47] B. O. Koopman. “Hamiltonian systems and transformation in Hilbert space”. In: *Proceedings of the National Academy of Sciences* 17.5 (1931), pp. 315–318. DOI: 10.1073/pnas.17.5.315.
- [48] J. v. Neumann. “Zur Operatorenmethode in der klassischen Mechanik”. In: *Annals of Mathematics* (1932), pp. 587–642. DOI: 10.2307/1968537.
- [49] R. Linares. “Koopman Operator Theory Applied to the Motion of Satellites”. In: *Advances in the Astronautical Sciences*. Vol. 171. AAS/AIAA. 2019, AAS 19–821. ISBN: 978-0-87703-665-4.
- [50] T. Chen and J. Shan. “Koopman-Operator-Based Attitude Dynamics and Control on SO (3)”. In: *Journal of Guidance, Control, and Dynamics* 43.11 (2020), pp. 2112–2126. DOI: 10.2514/1.G005006.
- [51] D. Arnas and R. Linares. “A set of orbital elements to fully represent the zonal harmonics around an oblate celestial body”. In: *arXiv preprint arXiv:2010.12722* (2020).